Graphite-superconductor junctions as a probe of order-parameter symmetry

David Parker[1] and Peter Thalmeier[2]
[1]*Max Planck Institute for the Physics of Complex Systems, Nöthnitzer Strasse 38, D-01187 Dresden, Germany*
[2]*Max Planck Institute for the Chemical Physics of Solids, Nöthnitzer Strasse 40, D-01187 Dresden, Germany*
(Received 7 June 2007; revised manuscript received 27 July 2007; published 22 August 2007)

We discuss a method for determining the order-parameter symmetry of quasi-one- and quasi-two-dimensional unconventional superconductors by the use of graphite-superconductor junctions. The use of a graphite gate voltage, in combination with a bias tunneling voltage, allows access to more information concerning gap values on the Fermi surface than with conventional tunneling spectroscopy, where only a bias voltage is employed. In particular, the use of a gate voltage allows one to tune the momentum-space size of the tunneling region, thus accessing gap values over local regions of the superconductor Fermi surface, in contrast to conventional tunneling techniques.

DOI: 10.1103/PhysRevB.76.064525 PACS number(s): 74.20.Rp

I. INTRODUCTION

Since the initial discovery of unconventional superconductivity in $CeCu_2Si_2$ by Steglich *et al.*,[1] much effort has centered on identifying the pairing state, or order-parameter symmetry, of superconducting materials. One highly useful tool has been low-temperature thermodynamics, such as specific heat and superfluid density and also nuclear spin relaxation rate and thermal conductivity. As is well known, in conventional superconductors these quantities generally display exponentially activated behavior, while in unconventional materials power-law behavior is observed. However, the only directionally sensitive probes, giving information about the angular position of nodes, currently in use are the magnetospecific heat and magnetothermal conductivity, as used by, e.g., Izawa *et al.*[2] and others. In these techniques, a sample's specific heat or thermal conductivity is measured in a magnetic field applied at various directions. The Doppler-shifted quasiparticles[3] yield information about the gap value when the gap value is less than the Doppler shift in quasiparticle energy.[4] This technique has been used as a powerful means for determining the likely location and type (point or line, first order or second order) of order-parameter nodes, and thereby finding the symmetry of the order parameter. Knowing this symmetry is of great value for understanding the mechanism of superconductivity in a given material.

In this paper, we propose a possible method for analyzing order-parameter symmetry that has the potential to yield information about the local value of the gap function at specific regions on the Fermi surface, not just the nodes.

II. PROPOSED METHOD

In the common tunneling setup, bias voltage V applied to the normal metal-insulator-superconductor (NIS) tunneling junction selects the energies of quasiparticles on the S side into which the normal electrons can tunnel. Quasiparticle momenta, however, are not selected and electrons with all possible momenta compatible with boundary conditions contribute to the tunneling current.

The basis of the method proposed here is the use of an additional gate voltage V_g applied to the N electrode to select the momentum range on the N side from which electrons can tunnel. A schematic setup is shown in Fig. 1. It shows the arrangement of superconductor, insulator layer, graphite electrode, and gate, along with the two voltages, gate (V_g) and tunneling bias (V). If a common metal is used as electrode, momentum selection is not possible because V_g changes the Fermi momentum only slightly. This is different if a semimetal electrode is applied where the relative change of k_F induced by V_g may be much bigger. Most suitable for this purpose would be an appropriately oriented graphite sheet (bc plane $\|$ to interface) acting as the N electrode in an NIS junction. Graphite has a very peculiar quasi-two-dimensional (quasi-2D) band structure which leads to narrow cigar- or rodlike Fermi surface sheets oriented along the k_z [HKH line in the three-dimensional Brillouin zone (BZ)].[5] A single graphite sheet (graphene) is a zero gap semiconductor with Dirac points at the corners of the hexagon BZ (which turn into H points in graphite). In graphite, the interplane hopping is much smaller than the in-plane hopping; therefore, slightly dispersive bands along HKH evolve from the Dirac point. For zero gate voltage V_g, the Fermi level is in the center of the flatband along k_z, resulting in the Fermi surface (FS) cigar spanning half the distance along HKH (Ref. 5) (see Fig. 2). Use of a positive or negative gate voltage V_g increases or decreases the length of the flatband cigar-shaped Fermi surfaces in the (001) direction, respectively, as

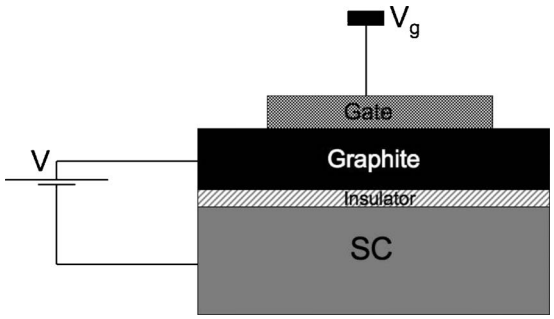

FIG. 1. Schematic drawing of the proposed NIS junction with layering arrangement of gate, graphite, insulator, and superconductor, with bias (V) and gate (V_g) voltages for energy and momentum selection of quasiparticles indicated, respectively.

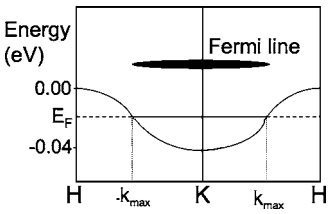

FIG. 2. A schematic diagram of the flatband centered at the K point, with the Fermi line at zero gate voltage indicated.

shown in Fig. 3. Changing the gate voltage from $-V_g^0$ to V_g^0 changes the length of the FS cigar from 0 to π/c, i.e., the whole length of the BZ along k_z.

Thus, when wave vector matching conditions at the boundary are applied, this method selects a specific, tunable region of the superconductor Fermi surface on which electrons propagate. The relevant normal material Fermi surface is effectively a set of rodlike Fermi lines running in the k_z direction. In the Blonder-Tinkham-Klapwijk (BTK) theory,[6] a differential tunneling conductance feature is usually observed at the gap magnitude. Given that in this proposed method one studies specific regions of momentum space, one observes a conductance feature at the local gap magnitude or at the gap feature occupying the largest region of phase space (on the superconductor Fermi surface) in a given geometry.

To make the issue clear, we have prepared diagrams of all the geometries to be used for this method, shown in Fig. 3. It shows a transverse and a longitudinal geometry. The top part of the figure shows the orientation of the graphite reciprocal cell, with the flatbands along the H-K line perpendicular to the nodes, which we have chosen to be vertical in this geometry. Several possible variations on this geometry, either by choosing horizontal nodes, rotating the graphite by 90°, or both, are clearly possible, and we note that a one-dimensional (1D) superconductor, with the superconducting Fermi cylinder replaced by a quasi-1D Fermi sheet, can also be used in all these geometries. For clarity, the top right figure shows the graphite-superconductor setup in real space; the graphite bc plane is the contact plane with the superconductor.

The bottom right figure shows a schematic diagram of a two-dimensional cylindrical Fermi surface in a longitudinal nodal configuration, with the longitudinal axis into the paper. In this geometry, there are two graphite Fermi lines, equally displaced from the origin in opposite directions, affecting the conductance. Due to the necessity of conserving momentum parallel to the interface (from the translational invariance in this direction), conductance will only occur at the four points where the graphite Fermi lines contact the cylindrical Fermi surface. This will happen at appropriately chosen bias voltages to tune the size of the Fermi line to the size of the superconducting Fermi cylinder, and will yield information about the local value of the gap at each of these four points. Given the number of cylindrical Fermi surface superconductors—the cuprates, $CeCoIn_5$, several organics—this technique could prove quite useful in determining the

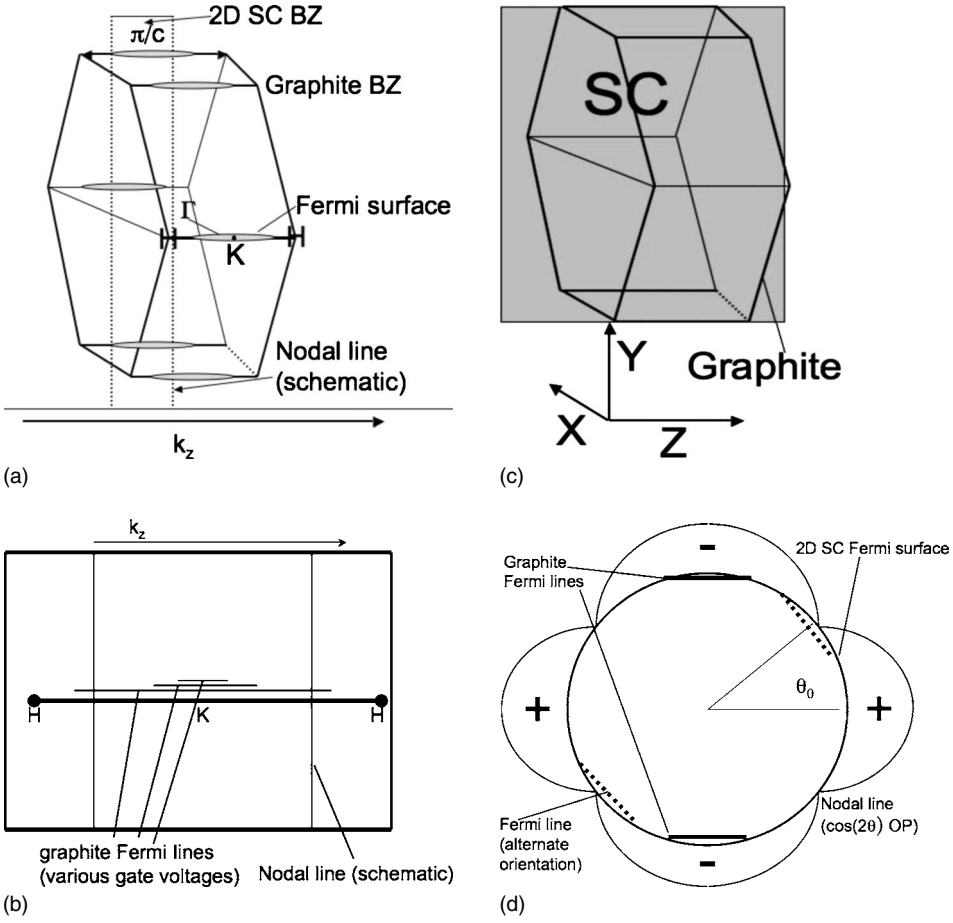

FIG. 3. The geometries for use in a graphite-superconductor junction. Top left: the graphite unit cell and a 1D or 2D Fermi surface. Top right: the top configuration in real space; note that the x-y axes are rotated 30° with respect to the momentum-space k_x-k_y axes. Bottom left: an expanded version of the top figure. Bottom right: the longitudinal 2D geometry, with the cylindrical Fermi surface perpendicular to the paper. Here, θ_0 is the relative angle between Cartesian coordinates on the N side (HKL plane) and S side (ab plane).

order-parameter symmetry of unconventional superconductors. $CeCoIn_5$, in particular, has had an ongoing controversy concerning whether its order parameter has $d_{x^2-y^2}$ or d_{xy} symmetry,[10] and an experiment in this configuration may be able to resolve this issue. We note that half the distance between the graphite Fermi lines must be nearly the same size as the $CeCoIn_5$ Fermi momentum (assuming a cylindrical Fermi surface[8]), or there will be no intersection (in parallel space) between the Fermi lines and the Fermi cylinder. Fortuitously, this is, in fact, the case; based on the $CeCoIn_5$ a-axis lattice constant of 4.62 Å,[9] we find $k_F=0.77$ Å^{-1} while half the Fermi line separation is 0.87 Å^{-1}.

We note that the above discussion will necessarily be complicated by multiband effects, particularly in the case where different gaps arise on different bands, and by three dimensionality, as is observed in some of the "115" materials (though not so much for $CeCoIn_5$). With regard to multiband effects, due to the conservation of parallel momentum, bands whose intersections with the Fermi surface are well separated (in momentum space) should not interact appreciably, and the gap structure on the band meeting the boundary conditions is the one that will be measured. Three dimensionality necessarily complicates measurements using the proposed technique, which is not generally well suited to such materials. However, the longitudinal configuration described above should still be effective for materials whose Fermi surface consists of an undulating cylinder, provided the nodal lines are parallel to the cylindrical axis and the parallel boundary conditions can be satisfied.

Finally, we note that based on the tight-binding fits for graphite,[7] there is a simple relationship between the length of the "cigar-type" Fermi surface oriented along HKH and the gate voltage V_g applied to the graphite. It is obtained by approximating the dispersion in Ref. 7 by

$$\varepsilon_k = \varepsilon_F - t_\perp \cos(2ck_z) + \frac{k_x^2 + k_y^2}{2m_N}, \tag{1}$$

where $t_\perp=0.02$ eV is the interlayer hopping and the Fermi level $\varepsilon_F=-0.02$ eV is at the band center which is chosen to adjust the Dirac point at H to zero energy. Furthermore, m_N is the in-plane effective band mass of graphite around the HKH line. The width of the FS cigar in the ab plane is given by $k_\parallel^0=(2m_N t_\perp) \ll \pi/a$. We neglect it in the following discussion and simply approximate the FS cigar by a Fermi line parallel to HKH. Its length for $V_g=0$ is given by $2k_{max}$ with $k_{max}=\frac{\pi}{2}\frac{1}{2c}$. Application of a positive or negative gate voltage will change the chemical potential to ε_F+eV_g. This leads to

$$k_{max} = \frac{1}{2c}\cos^{-1}\left(-\frac{eV_g}{t_\perp}\right) = \frac{1}{2c}\cos^{-1}(-50V_g), \tag{2}$$

with V_g measured in volts. Thus, changing the gate voltage V_g from $-V_g^0$ to $V_g^0=t_\perp/e$ sweeps the Fermi line from $k_{max}=0$ over the whole HKH line to the zone boundary $k_{max}=\frac{\pi}{2c}$ (the H point). This simple feature of the quasi-2D graphite band structure is utilized in the tunneling setup proposed above.

III. BOGOLIUBOV–DE GENNES EQUATION, COHERENCE FACTORS, AND CALCULATION FORMALISM

The microscopic state of a superconductor is described by the Bogoliubov–de Gennes (BdG) equations:[6,11–13]

$$i\hbar\frac{\partial f}{\partial t} = -\left[\frac{\hbar^2\left(\frac{\partial^2 f}{\partial x^2}+\frac{\partial^2 f}{\partial y^2}\right)}{2m_{xy}} + \frac{\hbar^2\frac{\partial^2 f}{\partial z^2}}{2m_Z} + \mu + V(x)\right] f(\mathbf{x},\mathbf{k},t) - \Delta(\mathbf{x},\mathbf{k})g(x,t), \tag{3}$$

$$i\hbar\frac{\partial g}{\partial t} = \left[\frac{\hbar^2\left(\frac{\partial^2 f}{\partial x^2}+\frac{\partial^2 f}{\partial y^2}\right)}{2m_N} + \frac{\hbar^2\frac{\partial^2 f}{\partial z^2}}{2m_Z} + \mu + V(x)\right] g(\mathbf{x},\mathbf{k},t) - \Delta(\mathbf{x},\mathbf{k})f(x,t). \tag{4}$$

We have written these equations in a form to make clear the different graphite effective masses. Strictly speaking, the m_Z for graphite is a function of wave vector, as the band is nonparabolic. However, this makes little difference in the formalism because the dispersion in this direction is already included in the energy in the coherence factors below.

The BdG equations have respective electron and hole solutions,

$$f(\mathbf{x},\mathbf{k},t) = u(\mathbf{k})\exp(i(\mathbf{k}\cdot\mathbf{r} - Et)/\hbar), \tag{5}$$

$$g(\mathbf{x},\mathbf{k},t) = v(\mathbf{k})\exp(i(\mathbf{k}\cdot\mathbf{r} + Et)/\hbar). \tag{6}$$

Here, u and v are the usual BCS coherence factors:[12,14,15]

$$u(\mathbf{k}) = \sqrt{\frac{1}{2}(1+\sqrt{E^2-|\Delta^2(\mathbf{k})|}/E)}, \tag{7}$$

$$v(\mathbf{k}) = \sqrt{\frac{1}{2}(1-\sqrt{E^2-|\Delta^2(\mathbf{k})|}/E)}. \tag{8}$$

We now study the process wherein an incoming electron in graphite undergoes Andreev[16] and normal reflection at the N-S interface. An electronlike quasiparticle and a backscattered holelike quasiparticle are transmitted to the superconductor, as shown in Fig. 2 of Ref. 17.

As in the original BTK work,[6] we have used a boundary delta-function potential $H\delta(\mathbf{x})$ to account for the usual existence of a narrow insulating layer between the superconductor and the graphite. As stated earlier, in general, translational invariance parallel to the interface dictates that the momentum in this direction be conserved. We note, however, the need for a smooth and well-defined graphite-superconductor interface to avoid random, diffusive scattering at the boundary, which would destroy the effectiveness of this method. To avoid repetition, we now refer the reader to our discussion of the setup and calculation of the Andreev reflection and normal reflection amplitudes a and b in Sec. III of Ref. 17.

Throughout, we take the dimensionless barrier parameter $Z=1$ and, for simplicity, assume equal effective masses on both sides of the barrier. The basic effect of unequal masses (for the case where $m_S \gg m_N$) is to reduce the subgap conductance and increase the coherence peak conductance, except for the cases containing a zero-bias conductance peak, where this peak is enhanced. Following BTK[6] and Tanaka and Kashiwaya,[13] the normalized conductance at temperature $T=0$ (which we assume throughout this paper) is given by

$$dI/dV = \sigma(V) \equiv \frac{\sigma_S(V)}{\sigma_N(V)} = \frac{\int_{\theta_1}^{\theta_2} \cos\theta d\theta (1 + |a(\theta,V)|^2 - |b(\theta,V)|^2)}{\int_{\theta_1}^{\theta_2} \sigma_N(\theta,V)\cos\theta d\theta}. \quad (9)$$

Here, θ is the angle of the quasiparticle momentum with the normal to the Fermi surface. For the quasi-1D and quasi-2D cases, where the Fermi surface is essentially a sheet located at a distance k_F from the origin of coordinates, $\theta_0=0$ and $\theta_1=\tan^{-1}(k_{max}/k_F)$. For the longitudinal 2D geometry (Fig. 3, bottom), the θ (polar angle) integration is replaced by a discrete sum over the azimuthal angle. As in Ref. 17, the only wave vectors that are of effect are the ones that lie on both the graphite Fermi line and the superconductor Fermi surface. We note that $k_\perp$ (direction across the boundary) is not conserved in this process and we make the simple assumption[18] that the system chooses the appropriate $k_\perp$ from the superconductor Fermi surface for transmission. We note that were this assumption untrue, no current would flow in the normal state, which is not likely to occur.

The key feature of this proposal is the use of a size-tunable Fermi surface, as is occasioned by voltage gates on the semimetal graphite. This allows substantially more information to be collected from a single experimental sample than in common tunneling experiments, where the FS geometry on the N side cannot be changed by a gate voltage.

IV. RESULTS

We note that the method is applicable to one- and two-dimensional materials. Also, to fully determine nodal structure, it is necessary that the length of the graphite "Fermi line" cover most of the length of the superconductor Brillouin zone. The distance from the graphite K point to the H point is approximately 0.44/Å, and setting this greater than or equal to the half Brillouin zone length $\frac{\pi}{c}$, where c is the c-axis lattice constant on the S side, yields $c \geq 7.1$ Å. Most of the organic superconductors[20] have c-axis lattice constants significantly greater than this value and so these materials appear to be suitable materials for the application of this technique.

In Figs. 4 and 5, we show the differential conductance numerically calculated for several unconventional order parameters which may be realized, e.g., in organic superconductors, in a configuration in which the Fermi line parallels a longitudinal cylindrical Fermi surface or a quasi-1D Fermi sheet. The first figure shows the result for $\Delta(\mathbf{k})=\Delta_0\cos(k_z)$. It is easily seen that the coherence peaks reduce in height as the Fermi line lengthens, and spectral weight is transferred toward energies away from the coherence peak. The peak itself, however, stays at the same energy. These results can be understood on the following basis: As the Fermi line lengthens, regions of smaller $\Delta_0\cos(k_z)$ are contributing to the tunneling conductance, so that more low-energy densities of states are observed. However, the maximum conductance is still found at $eV=\Delta_0$ because the order parameter is stationary at this point, so that more phase space (k_z) has $\Delta(\mathbf{k})$ values near the maximum Δ_0 than any other value, causing the peak.

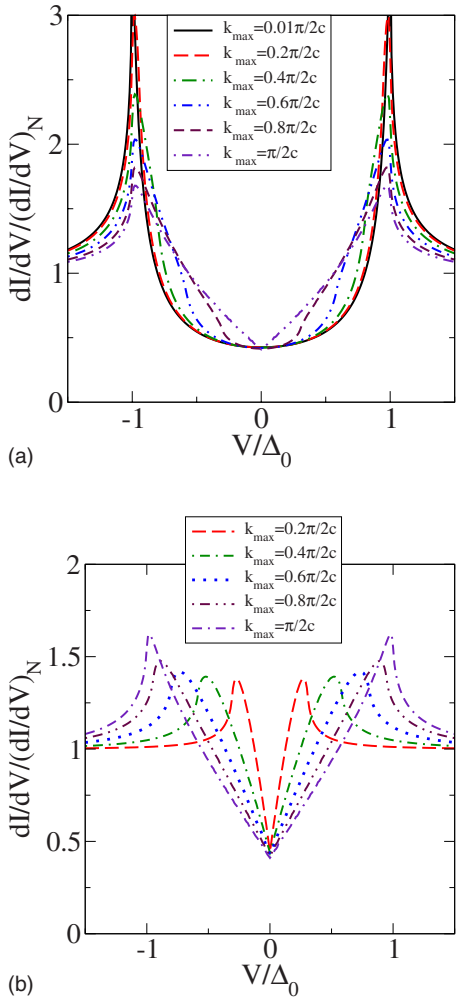

FIG. 4. (Color online) The differential conductance plots for varying graphite gate voltage are shown. From top: $\Delta_0\cos k_z$ and $\Delta_0\sin k_z$ (both: Fermi line $\|k_z$).

The second figure shows the result for $\Delta(\mathbf{k})=\Delta_0\sin(k_z)$. Here, the behavior is radically different from that of $\cos(k_z)$—the coherence peaks begin right at $V=0$ and move outward as the Fermi line lengthens, eventually reaching $eV=\Delta_0$ when the Fermi line reaches the antinodal line. A similar pattern occurs in the quasi-1D case $\Delta_0\sin(k_z)\sin(k_x)$

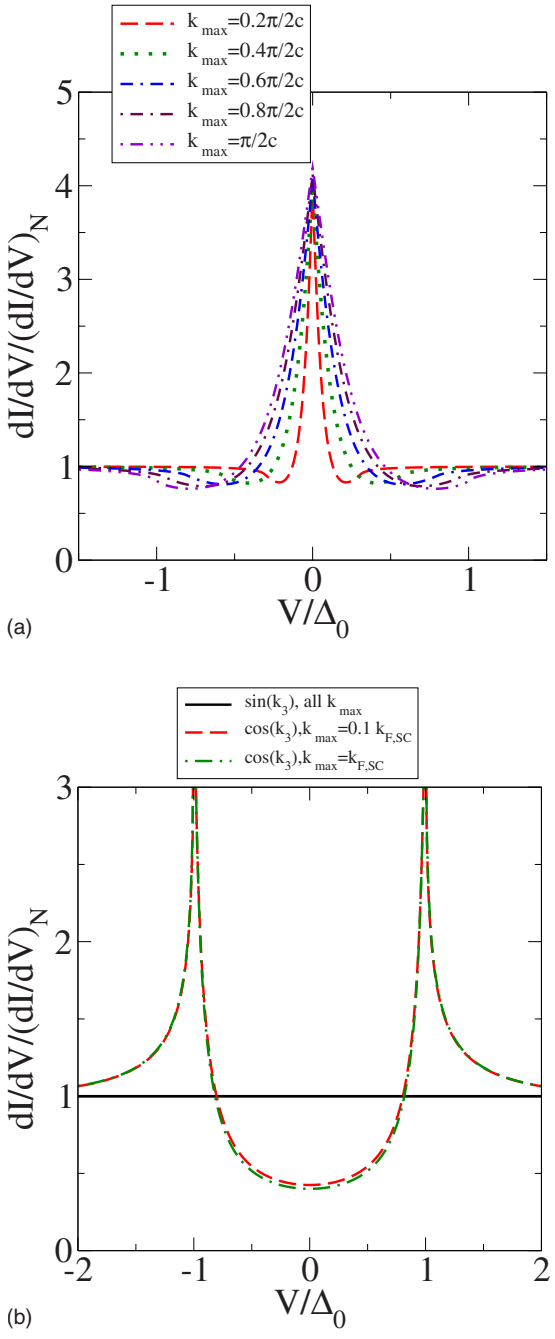

FIG. 5. (Color online) The differential conductance for varying gate voltages, for the order parameters (from top) $\Delta_0 \sin k_z \sin k_x$ (Fermi line $\| k_z$) and $\Delta_0 \cos k_z$ and $\Delta_0 \sin k_z$ (Fermi line $\perp k_z$).

(here, k_x refers to the perpendicular momentum from the origin of coordinates of two Fermi sheets). In this case, however, due to the sign change between the opposing sheets,[21] a zero-bias conductance peak is evident, which widens as the graphite Fermi line lengthens, as states of larger $\Delta(\mathbf{k})$ contribute to the conductance.

Finally, we have also plotted the results for $\Delta(\mathbf{k}) = \Delta_0 \sin(k_z)$ and $\Delta_0 \cos(k_z)$ in a transverse geometry wherein the graphite Fermi lines run perpendicular to the 2D Fermi cylinder. The result for $\Delta_0 \sin(k_z)$ is perhaps not too surprising—the entire Fermi line, regardless of its length,

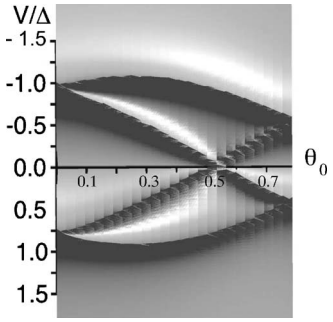

FIG. 6. The differential conductance in the longitudinal "into the paper" 2D configuration is shown, for the two order parameters $\Delta(\mathbf{k}) = \Delta_0 \cos(2\phi)$ and $\Delta_0 \sin(2\phi)$, as a function of the angle θ_0 (Fig. 3). For $\Delta_0 \cos(2\phi)$, the left side of the plot represents $\theta_0 = 0$ and the right side $\theta_0 = \pi/4$; for $\Delta_0 \sin(2\phi)$, these are reversed.

lies on the node and thus the tunneling conductance is that of the normal state. For the $\Delta_0 \cos(k_z)$ case, we observe that the conductance is essentially independent of the length of the graphite Fermi line, which is again a consequence of the constancy of the order parameter along the antinodal line matched by the graphite Fermi line.

In Fig. 6, we present the results of numerical calculations of $T=0$ differential conductance for the longitudinal 2D "into the paper geometry" with $\Delta(\mathbf{k}) = \Delta_0 \cos(2\phi)(d_{x^2-y^2})$ and $\Delta_0 \sin(2\phi)(d_{xy})$, where ϕ is the in-plane azimuthal angle from the x axis. These order parameters have been under discussion for some time now regarding the heavy-fermion superconductor $CeCoIn_5$. We have assumed here that the gate voltage has been chosen such that the graphite Fermi lines cross the 2D cylindrical Fermi surface, and have plotted the differential conductance when the graphite is oriented at various angles (θ_0) relative to the a axis of the superconductor. Clearly different behavior is observed for the two order parameters: for the $\Delta_0 \cos(2\phi)$ case, the coherence peaks for $\theta_0 = 0$ are at approximately 0.9 Δ_0, split and then move inward, terminating at $\theta_0 = \pi/4$ at approximately 0.5 Δ_0; the exact opposite is observed for $\Delta_0 \sin(2\phi)$. These patterns are sufficiently different that we believe that such an experiment, in which several graphite-$CeCoIn_5$ samples with various θ_0 were constructed, would help resolve the order-parameter controversy regarding this material.

The radically differing conductance curve sets for the seven order parameters studied make clear that the use of graphite-superconductor junctions is a potentially useful means of assessing order-parameter symmetry in unconventional superconductors. The essential feature of all these results is that more order-parameter information is available with a single graphite-superconductor experiment than with more conventional tunneling spectroscopy due to the use of a size-tunable Fermi line in the graphite.

V. CONCLUSION

In summary, we propose a method for order-parameter determination in unconventional superconductors based on

the use of graphite as the normal electrode, with a gate voltage applied to tune the size of the occupied graphite Fermi surface. We have shown that this method can be expected to yield more information than conventional tunneling spectroscopy, and that even the most common order parameters can be expected to display widely divergent behavior when investigated using this method. We may therefore expect that this technique may become a useful tool for determining order-parameter symmetry.

ACKNOWLEDGMENTS

We are pleased to acknowledge the assistance of J. Müller, I. Eremin, and B. Dora in reading the paper prior to submission.

[1] F. J. Steglich, J. Aarts, C. D. Bredl, W. Lieke, D. Meschede, W. Franz, and H. Schäfer, Phys. Rev. Lett. **43**, 1892 (1979).
[2] K. Izawa, Y. Kasahara, Y. Matsuda, K. Behnia, T. Yasuda, R. Settai, and Y. Onuki, Phys. Rev. Lett. **94**, 197002 (2005); K. Izawa, Y. Nakajima, J. Goryo, Y. Matsuda, S. Osaki, H. Sugawara, H. Sato, P. Thalmeier, and K. Maki, *ibid.* **90**, 117001 (2003).
[3] G. E. Volovik, JETP Lett. **58**, 496 (1993).
[4] H. Won, S. Haas, D. Parker, S. Telang, A. Ványolos, and K. Maki, *Lectures on the Physics of Highly Correlated Electron Systems IX*, AIP Conf. Proc. No. 789 (AIP, New York, 2005).
[5] A. Grüneis, C. Attaccalite, T. Pichler, V. Zabolotnyy, H. Shiozawa, S. L. Molodstov, D. Inosov, A. Koitzsch, M. Knupfer, J. Schiessling, R. Follath, R. Weber, P. Rudolf, L. Wirtz, and A. Rubio, arXiv:0704.2682 (unpublished).
[6] G. E. Blonder, M. Tinkham, and T. M. Klapwijk, Phys. Rev. B **25**, 4515 (1982).
[7] B. Partoens and F. M. Peeters, Phys. Rev. B **74**, 075404 (2006).
[8] T. Maehira, T. Hotta, K. Ueda, and A. Hasegawa, J. Phys. Soc. Jpn. **72**, 854 (2003).
[9] C. Petrovic, P. G. Pagliuso, M. F. Hundley, R. Movshovich, J. L. Sarrao, J. D. Thompson, Z. Fisk, and P. Monthoux, J. Phys.: Condens. Matter **13**, L337 (2001).
[10] K. Izawa, H. Yamaguchi, Y. Matsuda, H. Shishido, R. Settai, and Y. Onuki, Phys. Rev. Lett. **87**, 057002 (2001).
[11] P. G. deGennes, *Superconductivity of Metals and Alloys* (Addison-Wesley, Reading, 1989).
[12] T. M. Klapwijk, G. E. Blonder, and M. Tinkham, Physica B & C **109-110**, 1657 (1982).
[13] Y. Tanaka and S. Kashiwaya, Phys. Rev. Lett. **74**, 3451 (1995).
[14] C. Honerkamp and M. Sigrist, J. Low Temp. Phys. **111**, 895 (1998).
[15] J. R. Schrieffer, *Theory of Superconductivity* (Perseus, Reading, 1999).
[16] A. F. Andreev, Sov. Phys. JETP **19**, 1228 (1964).
[17] D. Parker and P. Thalmeier, Phys. Rev. B **75**, 184502 (2007).
[18] This assumption is at odds with that made in Ref. 19; however, in that work a spherical Fermi surface and parabolic dispersion (constant effective mass) were assumed, neither of which applies here.
[19] N. A. Mortensen, K. Flensberg, and A.-P. Jauho, Phys. Rev. B **59**, 10176 (1999).
[20] D. Jérome and H. J. Schulz, Adv. Phys. **51**, 293 (2002).
[21] K. Sengupta, I. Zŭtić, H.-J. Kwon, V. M. Yakovenko, and S. Das Sarma, Phys. Rev. B **63**, 144531 (2001).